International Journal of Engineering & Technology, 7 (2) (2018) 891-896

International Journal of Engineering & Technology

Website: www.sciencepubco.com/index.php/IJET
doi: 10.14419/ijet.v7i2.10901
Research paper

Nano indentation and morphology study of the polypropylene and high density polyethylene nanocomposites based on exfoliated graphite Nano platelets/Nano-magnesium oxide

A. I. Alateyah *

Qassim university, Unaizah Engineering College, Qassim, Kingdom of Saudi Arabia
**Corresponding author E-mail: aialateyah@gmail.com*

Abstract

Polypropylene (PP) and high density polyethylene (HDPE) were successfully fabricated using injection molding machine, by the addition of exfoliated graphite nanoplatelets composites reinforced with 2wt.t% of nano-magnesia. The nanoindentation properties and microstructure of the composites were investigated, in the current study. The XRD patterns of both composites showed the peaks of xGnP and n-MgO, where their intensity became stronger with increasing the concentration of xGnP added into both polymers. In addition, the SEM micrographs revealed a good dispersion of fillers within the matrix. The nanoindentation properties of both nanocomposites revealed better properties with compared to the virgin polymers. The PP nanocomposites showed an improvement of hardness up to 22 % and 118% with the compositions of 1xGnP/2n-MgO and 5xGnP/2n-MgO respectively. In addition, HDPE/1xGnP/2n-MgO and HDPE/5xGnP/2n-MgO represented a dramatic improvement of hardness up to 146% and 341% respectively with compared to virgin polymer. In addition, the enhancements in reduced modulus of PP and HDPE were proportional to the xGNP loading.

Keywords: *Polypropylene; High Density Polyethylene; Exfoliated Graphite Nanoplatelets; Magnesium Oxide Nanoparticles; Nanoindentation, XRD; SEM.*

1. Introduction

Several advantages of thermoplastic composites over classical thermoset-based matrices composites made them a main point of interest. The benefits vary from environmental such as the superior recyclability tendency, practicality like the processing easiness and lightweight, in addition to the low cost [1-6].

One of the most utilized types of thermoplastic resins in industrial applications is the Polypropylene (PP), which is used in automotive industry, packaging, non-structural applications, and many others [7]. The urge to benefit from the extraordinary features of PP lead to the focus on its enhancement, by seeking suitable techniques of reinforcement, which is revealed in novel presented matrices like carbon nanotubes[8], carbon black [9], and graphite [10]. On the other hand, high density polyethylene (HDPE) is another commonly used thermoplastic in industry, thanks to its superior physical and mechanical properties. However, the adoption of HDPE in structural application is limited due to the need for better mechanical properties, which is an active point of improvement that could be accomplished with the introduction of several additives like glass fiber, carbon fiber, and carbon black [11].

Nowadays, the urge to obtain better enhanced properties led to the focus on novel filler types in polymeric matrices. The exfoliated graphite nanoplatelets (xGnPs) is an extraordinary promising reinforcement filler distinguished with its character of being semi-metallic, which usually contains up to nine graphene layers reaching a total thickness of only few nanometers and few 100 μm for the other two dimensions [11-17]. As a result of its superior potential, the adoption of xGnP as a reinforcement to ameliorate the electrical, mechanical, and thermal properties has been on the rise [18], [19].

Likewise, magnesium oxides (MgOs) Nanoparticles are vastly adopted metal oxides, which could be highly tempting potential filler. They are known to be obtained from various low-cost raw materials including magnesium salts, bearing minerals, and brines; moreover, they are characterized with outstanding properties like their remarkable thermodynamic stability, noticeably elevated hardness, melting point, strength, and modulus [20].

Nanoindentation is a fairly new advance technique, which can provide with valuable and accurate quantitate information about the mechanical behavior of different materials at an initial surface layers. The method of nanoindentation depends on a local deformation that presented on a materials surface by utilizing an indenter with specific geometry under a given load. In this method, a combination of both the viscoelastic and viscoplastic properties which relies on the total indentation depth. In addition, the yield stress in the nanoindentation method is exceeded. In summary, this method could provide more useful information of nanocomposites materials, and allow people get fundamental understanding of the nanocomposite properties [21], [22].

It is worth mentioning that there are very limited attempts in literature to work with MgO as a Nano-filler added into HDPE and PP, based on composites of xGnPs. As a result, the main aim of the work presented in this paper is the investigation of nanoindentation properties of PP and HDPE based on xGnP/n-MgO composites, where indentation experiments were adopted for the meas-

urement of materials' hardness and quantifying their resistance to plastic deformation. Vickers hardness test was used, due to its scale capabilities for hardness measurement for both ceramic and metallic materials [23].

2. Experimental procedures and methods

2.1. Materials

N-MgO and xGnP with a 99.9% purity, provided by Tritrust Industrial Co in China, were utilized as filler materials in this work. The adopted particle sizes of n-MgOs and xGnP averaged around 100 nm and 10 μm, respectively, and the thickness of the latter was 5 nm. Moreover, HDPE and PP in a granular form were supplied by SABIC, Kingdom of Saudi Arabia.

2.2. Fabrication of composites

The process of the fabrication of composites in this work begins with the adoption of an analytical balance to weigh the HDPE, PP, n-MgOs, and xGnP with fixed compositions, as shown in Table **1**.

Table 1: Composition Of Composites (All In Weight %)

Sample	PP (wt.%)	HDPE (wt.%)	xGnPs (wt.%)	N-MgO (wt.%)
100 wt. % PP	100	0	0	0
PP/ 1xGnP/2n-MgO	97	0	1	2
PP/ 5xGnP/2n-MgO	93	0	5	2
100 wt. % HDPE	0	100	0	0
HDPE/ 1xGnP/2n-MgO	0	97	1	2
HDPE/ 5xGnP/2n-MgO	0	93	5	2

The next step was the utilization of a mechanical disperser to perform a mixing process for the above weighed powders, aiming at reaching a temporary state of homogeneity. Hence, the resulted mix was placed into a special injection molding machine, Battenfeld HM 1000/750, to produce the required samples. The machine was characterized during the process with a 10-ton force of clamping, 22 L/D ratio, 45 mm for the screw diameter, 230°C for the barrel and nozzle temperature, 3000 psi for the pressure, and 20°C for the mold temperature. The outcome samples were divided into 6 dissimilar compositions, shown in Table 1, aiming to be tested for the detection of the effect on nanoindentation properties of PP-xGnP composites when adding n-MgOs as well as HDPE- xGnP/ n-MgOs.

2.3. Characterization

2.3.1. X-Ray diffraction analysis

The nanocomposites' compositions and definitions of the existing phases were checked utilizing X-ray diffraction (XRD). The characteristics of nanoparticles were provided through wide-angle X-ray diffraction (WAXD) patterns, with the adoption of an X-ray diffractometer equipped with a CuKα radiation. Survey scan operated in a range of 10° to 90°, with a scanning speed of two° per minute.

2.3.2. Scanning electron microscopy (SEM)

The setting up of samples was done by fracturing (cryo- fracturing) the sample cutting into pieces of 1 cm long, from the neck portion of tensile samples, and attaching them to Al stubs with 12.5 mm in diameter, having sticky C tabs of 12 mm in diameter. Consequently, the samples were taken to be coated for 1 to 2 minutes with Au-Pd sputter coating, at a partial pressure of ~0.1 torr for Ar, and a deposition current of 25 mA. Afterwards, An SEM examination for the samples was taking place according to the shown setup in Table 2.

Table 2: Setup Conditions of SEM Used for Microstructural Observation.

Instrument	HV, kV	WD, mm	Spot Size	Image Modes	Image Resolution
FEI Quanta 200 (SEM-2)	20.0	15-25	3.0	SEI	1024 x 784

3. Test

3.1. Nano indentation

NanoTest (Micro Materials, UK) was the utilized device to perform all the required nanoindentation tests in this work, where a Berkovich (three-sided pyramidal) diamond indenter tip was used to accomplish 12 identical indentations on each sample, creating a matrix with 30 μm apart. Injection molding process was adopted to obtain nanocomposites with particular dimensions of 20 × 80 × 3 mm, approximately, from which test coupons were cut to be consequently fixed onto the nanoindentation fixture by means of an appropriate suitable adhesive. The following are the adopted parameters for all measurements: a loading and unloading rate (strain rate) of 2.00 mN/S, dwell time or holding time at maximum load of 5 s, and initial and maximum load for all indents of 0.1 mN and 5 mN, respectively.

3.2. Hardness and elastic modulus

Hardness is defined as the measurement means for the resistance to deformation or damage [22], which is calculated, in the case of nanoindentation test, through the determination of the project area of contact and the peak load as shown in Eq. (1). Moreover, the calculation of the reduced modulus could be done by knowing the unloading portion of the indentation depth and the elastic modulus could be calculated, as shown in Eq. (2) [24]. In addition, the calculation of the elastic modulus can be done using Eq. (3).

$$\mathrm{H} = \frac{\mathrm{Pmax}}{\mathrm{Ac}}$$

$$\frac{\mathrm{E}}{1-\mathrm{V}^2} = \frac{\sqrt{\pi}}{\mathrm{Z}} \frac{1}{\sqrt{\mathrm{Ac}}} \mathrm{S}$$

Where V, Pmax, Ac, and S are the Passion's ratio, the driving force of the indenter, contact area at the time that the material is in contact with the indenter with the load P max, and material stiffness, respectively.

$$E_s = \frac{(1-V_s)^2}{\frac{1}{E_r} - (1-\upsilon_i)^2/E_i}$$

Where
V_s ,E_s,V_i,E_i, and E_r are the sample Poisson's ratio (approximately valued at 0.42 for both polymers), the elastic modulus, the indenter Poisson's ratio (valued at 0.07 for diamond), the indenter elastic modulus (valued at 1141 GPa for diamond), and the reduced modulus, respectively.

4. Results and discussions

4.1. Characterizations

4.1.1. XRD

A commonly utilized technique in the determination of composites characterization is the Wide Angle X-ray Diffraction (WAXD), which is known to be used in studying intercalation or exfoliation

structures. The process is accomplished through calculating the inter-gallery spacing, which are responsible for recognizing the structures of composites [22]. Therefore, the d-spacing amount of the inter-gallery could be identified for a various particles loading composites, in addition to neat polymers.

Fig. **1** shows the XRD patterns of the neat PP and PP/xGnP composites with various compositions of fillers, where xGnP and n-MgO were presented in the samples from 1 to 3. xGnP peaks could be clearly detected in the two theta of 26.6^0 in all composite samples, which matches the results published in a previous work published by Geng et al. [25]. Moreover, the n-MgO was observed at the two theta of 42.9^0, which suggests a face centered cubic crystalline phase (JCPDS No 45-0496) [26]. In addition, the intensity of the xGnP peaks became stronger with increasing its concentration into PP matrix, whereas the intensity of n-MgO was relatively persistent as observed in Fig. **1**. Table 3 represents the change of the basal spacing (d001 spacing) of the composites, which was calculated by Bragg's Law using the values extracted from the XRD patterns, according to a paper published earlier by Shen et al. [25]. On the other hand, Fig. **2** showed almost the same pattern for the xGnP peaks of HDPE polymers, where the increase of xGnP led to an increase in the intensity of xGnP peaks.

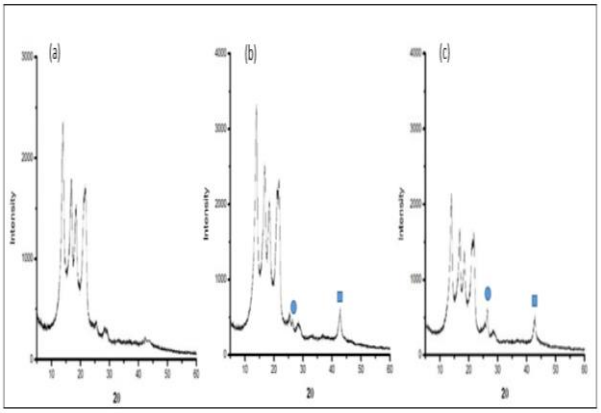

Fig. 1: XRD Curves of PP and Its Composites: (A) 100 Wt. Percentage PP, (B) PP/ 1xgnp/2n-Mgo, (C) PP/ 5xgnp/2n-Mgo.

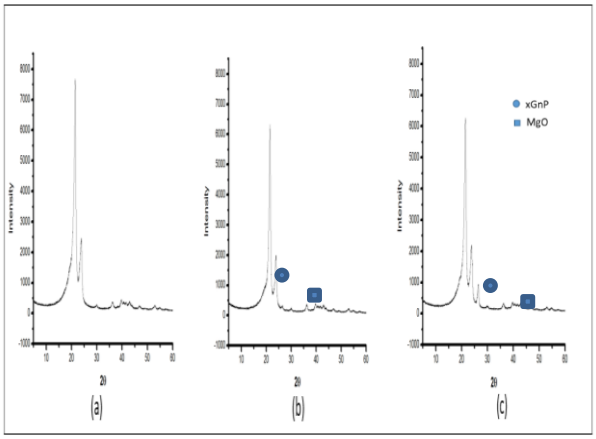

Fig. 2: XRD Curves Of HDPE and its Composites: (A) 100 Wt. Percentage HDPE, (B) HDPE/ 1xgnp/2n-Mgo, (C) HDPE/ 5xgnp/2n-Mgo.

Table 3:XRD D-Spacing of Various PP and HDPE Nanocomposites Samples.

Samples	2 Theta	d-spacing [Å]
100 wt. % PP	21.87	4.06
PP/ 1xGnP/2n-MgO	21.03	4.22
PP/ 5xGnP/2n-MgO	21.75	4.08
100 wt. % HDPE	21.48	4.13
HDPE/ 1xGnP/2n-MgO	21.50	4.12
HDPE/ 5xGnP/2n-MgO	21.52	4.12

4.2 Scanning electron microscopy (SEM)

Figure-3 shows the SEM micrographs for the PP and various composites of n-MgO and xGnP, where the neat PP microstructure sample, as seen in Fig. **3**a, exhibited a structure similar to a wave form explaining its distinctive characteristic. On the other hand, the dispersion of filler particles within the PP matrix, as seen in Fig. **3**b and 3c, showed an adequate dispersion and are almost embedded into matrix; moreover, their interfaces looks bonded effectively. Therefore, nanoindentation properties of composites are estimated to be ameliorated; on the other hand, traces of agglomerations could be seen in Fig. **3**c in the samples with 5 wt. % xGnP addition.

The intercalation level was nearly attained, as shown in

(A)

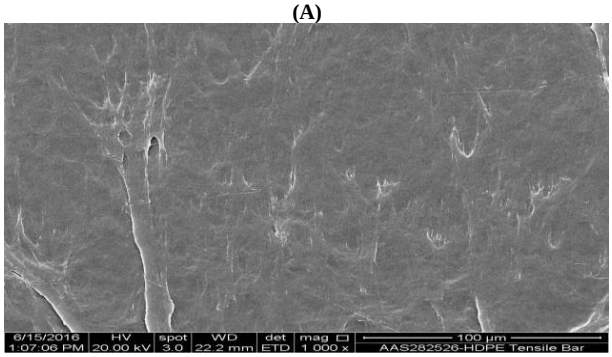

(B)

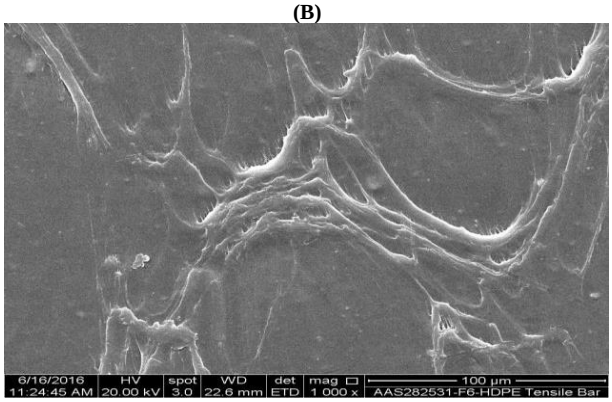

(C)

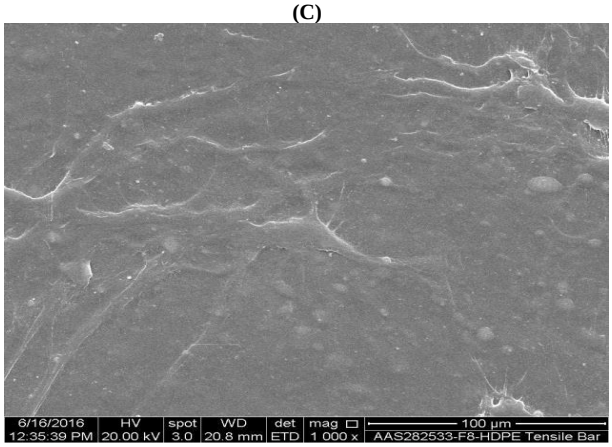

Fig. 4 of SEM images, for the HDPE and corresponding nanocomposites. Inversely, less intercalation level was obtained in both polymers with the addition of 5 wt.% xGnP, which could be associated with particles' agglomeration or the possibility of having lost platelet morphology of xGnP, leading to a development of roll up structure or folds throughout preparation, causing dispersion differences [11]. It is worth mentioning that reaching homogeneous dispersion is the most challenging obstacle to obtain an efficient reinforced polymer, especially in the case of non-polar polymers such as polypropylene (PP) [22], [27].

(A)

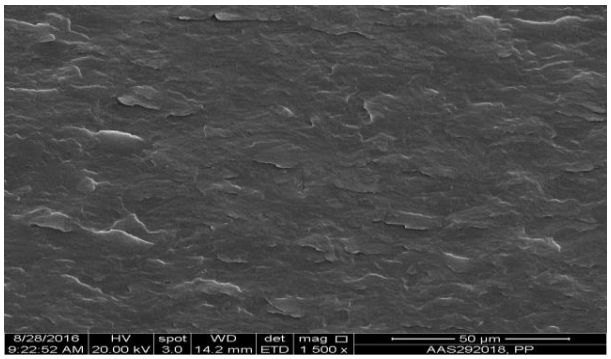

(B)

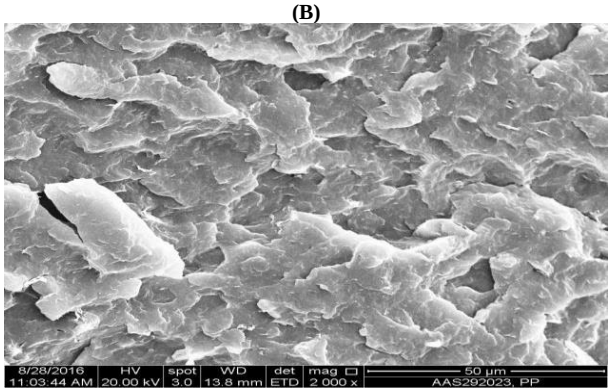

(C)

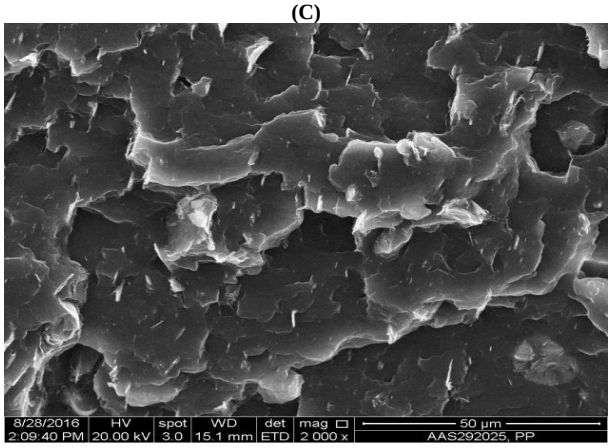

Fig. 3: SEM Images of (A) PPG0M0, (B) PPG1M2, and (C) PPG5M2.

(A)

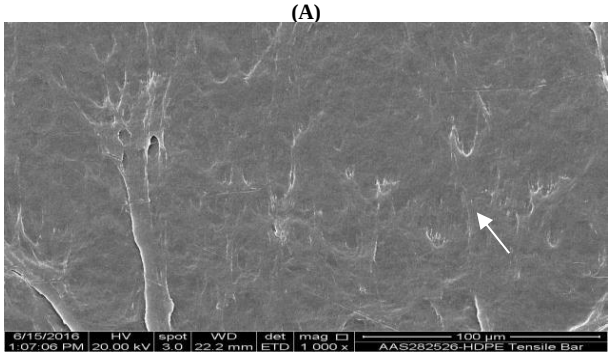

(B)

xGNP

xGNP

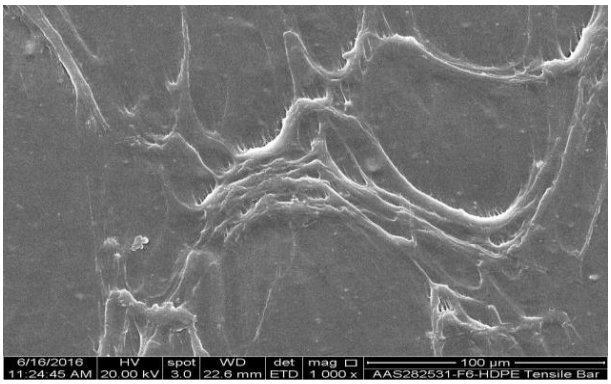

(C)

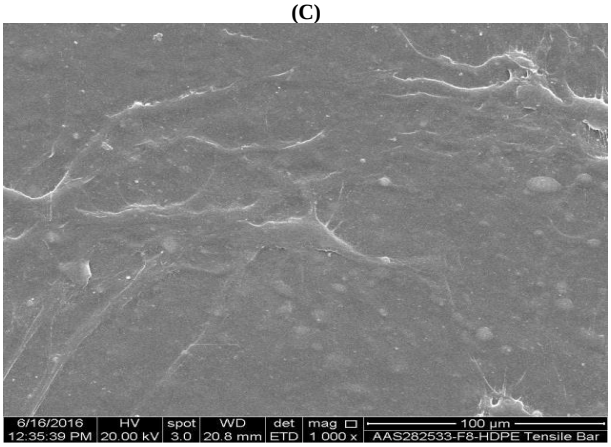

Fig. 4: SEM Images of (A) HDPEG0M0, (B) HDPEG1M2 and (C) HDPEG5M2.

4.3. Test

4.3.1. Nano indentation

Table 4: Nano indentation Behavior of the Neat PP, HDPE, and Their Corresponding Nanocomposites (Extracted from the Load-Unload Curve of the Experimental Nano indentation Test)

Samples	Max Depth (nm) (SD)	Hardness (Gpa) (SD)	Reduced modulus (Gpa) (SD)
PPG0M0	2003.863 (+34)	0.064 (+0.003)	1.35 (+0.039)
PPG1M2	1809.128 (+21)	0.078 (+0.002)	1.6 (+0.013)
PPG5M2	1380.005 (+52)	0.139 (+0.009)	2.5 (+0.19)
HDPEG0M0	2257.762 (+94)	0.048 (+0.005)	1.22 (+0.13)
HDPEG1M2	1446.185 (+101)	0.118 (+0.02)	2.94 (+0.063)
HDPEG5M2	1141.188 (+73)	0.212 (+0.54)	3.23 (+0.04)

The experimental data mean results obtained from the curves of loading unloading for nanoindentation tests are shown in **Error! Reference source not found.**. Fig. **5** displays the relationship between the load-depth curve of neat PP and the corresponding nanocomposites with various n-MgO and xGnP concentrations. It was noted that a gradual improvement was reached in the nanocomposites' hardness when adding xGnP to the PP, in comparison with neat polymer, which exhibited the least hardness of 0.064 GPa and highest indentation depth of 2003.863 nm. On the other hand, a hardness improvement to 0.078 GPa and reduction in indentation depth to 1809.128 nm were reached with adding 2% of n-MgO and 1% of xGnP. Moreover, reaching an addition of 2% n-MgO and 5% of xGnP led to a hardness of 0.139 GPa with an approximate improvement of 118% and maximum indentation depth of 1380.005 nm. Looking at Fig. **6**, it displays another relationship between the load-depth curve of neat HDPE and the corresponding nanocomposites with various concentrations of xGnP and n-MgO. The virgin HDPE showed the highest indentation depth of 2257.762 nm and the least hardness of 0.048 GPa, compared to polymer matrix. Adding 2% of n-MgO and 1% of xGnP led to a hardness improvement of about 145%, compared to the neat HDPE, and reduction in indentation depth to 1446.185 nm. Moreover, adding 2% of n-MgO and 5% of xGnP led to a 341%

of hardness amelioration and decrease of max depth to 1141.188 nm. Therefore, it could be concluded that nanocomposites samples, of both polymers, showed dramatic hardness amelioration compared to the neat polymer.

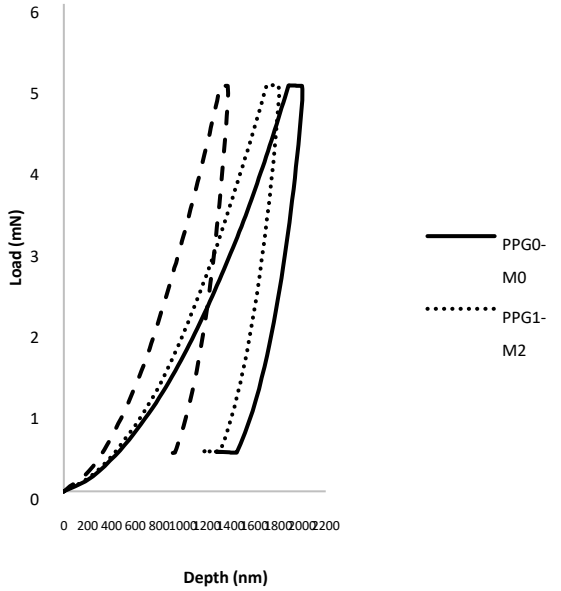

Fig. 5: The Relationship between the Load (Mn), the Max Depth (Nm) of the Neat PP, and the Corresponding Nanocomposites.

The obtained results by SEM and XRD could be interpreted as a clear indication of the well dispersion of fillers through the matrix, leading to structures of nanocomposites which are intercalated or intercalated partially exfoliated. Moreover, as the definition of hardness implies, hardness amelioration is an increase of material resistance to plastic deformation, which entitles that adding xGnP and n-MgO has a strong correlation with the alteration in material's behavior, under the plastic deformation. The results showed that a left shift took place in the PP and HDPE curves when adding xGnP and 2% of n-MgO, which showed an increase in resistance to indention for the samples of nanocomposites. The amelioration in hardness was detected through the aspect ratio of nano fillers particles.

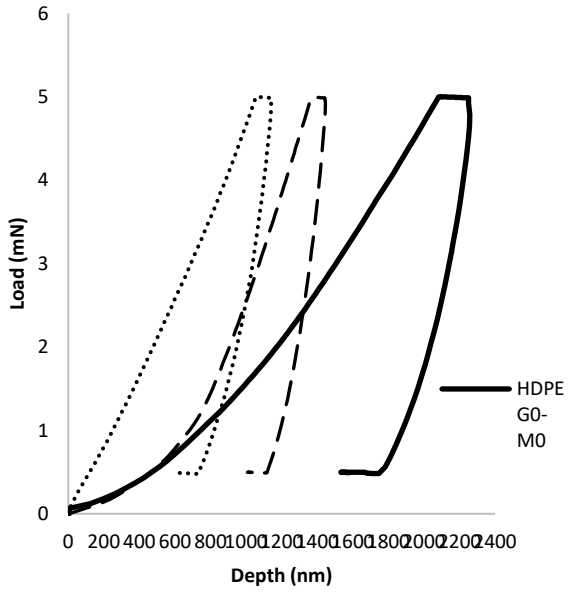

Fig. 6: The Relationship between the Load (Mn), the Max Depth (Nm) of the Neat HDPE, and the Corresponding Nanocomposites.

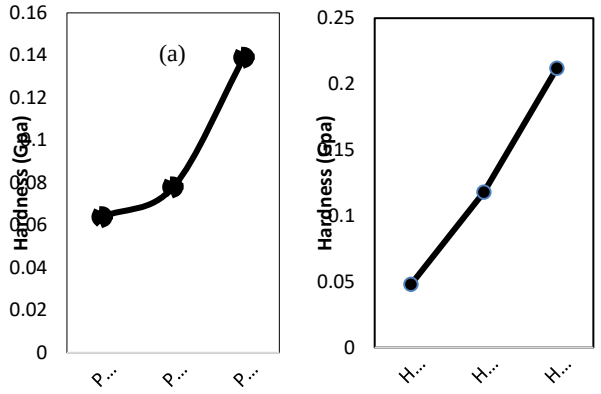

Fig. 7: Hardness Properties of Different Composition of (A) PP and (B) PE.

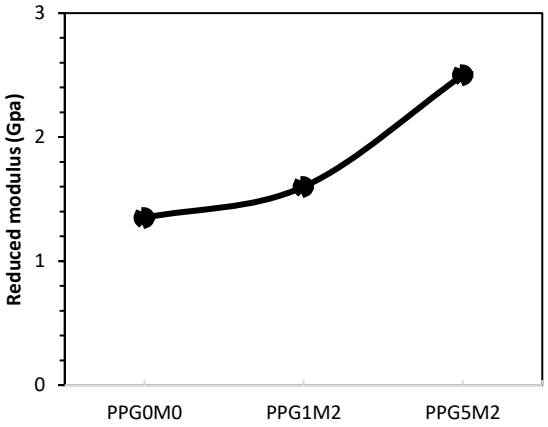

Fig. 8: Reduced Modulus of the PP and the Corresponding Nanocomposites.

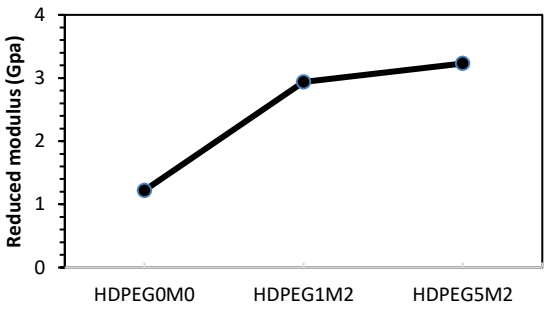

Fig. 9: Reduced Modulus of the HDPE and the Corresponding Nanocomposites.

The obtained reduced modulus of the neat PP was 1.35 GPa; whereas adding 2% of n-MgO and 1% of xGnP to the PP matrix ameliorated the reduced modulus to 1.6 GPa. Moreover, a reduced modulus valued up to 2.5 GPa was achieved with adding 2% of n-MgO and 5% of xGnP. On the other hand, HDPE reduced modulus showed alike pattern as the PP, where the neat HDPE resulted in a modulus of 1.22 GPa, which is less than the counterparts of HDPE matrix with the addition of n-MgO and xGnP, where 2% of n-MgO and 1% of xGnP lead to 2.94 GPa and increasing the xGnP to 5% resulted in 3.23 GPa. Therefore, it could be concluded that the reduced modulus showed proportionality with adding n-MgO and xGnP, as shown in Fig. **8** and Fig. **9** .

The interpretation of the increased modulus could be associated with the stiff fillers added to the matrices of polymers; moreover, adding nano fillers constrains the chain mobility of the PP and HDPE matrix under load, leading to ameliorated modulus. In addition, the direction of the nano fillers chain has a crucial role in modulus improvement. On the other hand, equation (3) was used to calculate the elastic modulus of the neat polymers and the cor-

responding samples, leading to similar results of the elastic and reduced modulus, as shown in Table 5.

Table 5: Elastic Modulus

Samples	Reduced modulus (GPA)
PPG0M0	1.14
PPG1M2	1.35
PPG5M2	2.10
HDPEG0M0	1.03
HDPEG1M2	2.47
HDPEG5M2	2.72

5. Conclusion

The PP/xGNP-MgO/PP and HDPE/xGNP-MgO nanocomposites were successfully fabricated using injection molding machine, which was proven to be an effective way to disperse particles into the polymers' matrices. The combinations of nanocomposites exhibited remarkable improvement in hardness properties. The XRD and SEM showed the intercalation levels of various compositions and explained the impact of the exfoliation levels on the properties. The hardness of neat PP and HDPE exhibited only 0.064 GPa and 0.048 GPa. However, the addition of 1 wt. t % of xGNP and 2% of n-MgO into PP and HDPE matrix resulted in increasing the hardness up to 0.078 GPa and 0.118 GPA respectively. By the incorporation of 5wt. t % of xGNP and 2wt.t% of n-MgO, the PP and HDPE nanocomposites represented 0.122 GPa and 0.323 GPa. In addition, the improvements in reduced modulus of PP and HDPE were proportional to the xGNP loading. In conclusion, all samples of nanocomposites showed enhanced hardness and reduced modulus compared to the neat polymers, which verifies the success of the fabricated nanocomposites.

Acknowledgement

The authors would like to thank and appreciate the effort of SABIC for their sustainable support and tremendous help and contribution, in the preparation of composites and its characterizations.

References

[1] N. Zhao, H. Rödel, C. Herzberg, S.-L. GAO, and S. Krzywinski, "Stitched glass/PP composite. Part I: Tensile and impact properties," *Composites Part A: Applied Science and Manufacturing*, vol. 40, no. 5, pp. 635-643, 2009. https://doi.org/10.1016/j.compositesa.2009.02.019.

[2] M. Tufail, "Processing investigation and optimization for hybrid thermoplastic composites," *Journal of University of Science and Technology Beijing, Mineral, Metallurgy, Material*, vol. 14, no. 2, pp. 185-189, 2007. https://doi.org/10.1016/S1005-8850(07)60036-X.

[3] C. Chuai, K. Almdal, L. Poulsen, and D. Plackett, "Conifer fibers as reinforcing materials for polypropylene-based composites," *Journal of Applied Polymer Science*, vol. 80, no. 14, pp. 2833-2841, 2001. https://doi.org/10.1002/app.1400.

[4] C. Albano, J. Gonzalez, M. Ichazo, and D. Kaiser, "Thermal stability of blends of polyolefins and sisal fiber," *Polymer Degradation and Stability*, vol. 66, no. 2, pp. 179-190, 1999. https://doi.org/10.1016/S0141-3910(99)00064-6.

[5] A. Long, C. Wilks, and C. Rudd, "Experimental characterisation of the consolidation of a commingled glass/polypropylene composite," *Composites Science and Technology*, vol. 61, no. 11, pp. 1591-1603, 2001. https://doi.org/10.1016/S0266-3538(01)00059-8.

[6] A. Shalwan, A. Alateyah, B. Aldousiri, and M. Alajmi, "Thermal and Nanoindentation Behaviours of Layered Silicate Reinforced Recycled GF-12 Nanocomposites," *Journal of Materials Science Research*, vol. 5, no. 4, p. 10, 2016. https://doi.org/10.5539/jmsr.v5n4p10

[7] H. M. Da Costa, V. D. Ramos, and M. C. Rocha, "Analysis of thermal properties and impact strength of PP/SRT, PP/EPDM and PP/SRT/EPDM mixtures in single screw extruder," *Polymer Testing*, vol. 25, no. 4, pp. 498-503, 2006. https://doi.org/10.1016/j.polymertesting.2006.02.003.

[8] L. Zhang, M. Kai, and K. Liew, "Evaluation of microstructure and mechanical performance of CNT-reinforced cementitious composites at elevated temperatures," *Composites Part A: Applied Science and Manufacturing*, vol. 95, pp. 286-293, 2017. https://doi.org/10.1016/j.compositesa.2017.02.001.

[9] T. Gong, S.-P. Peng, R.-Y. Bao, W. Yang, B.-H. Xie, and M.-B. Yang, "Low percolation threshold and balanced electrical and mechanical performances in polypropylene/carbon black composites with a continuous segregated structure," *Composites Part B: Engineering*, vol. 99, pp. 348-357, 2016. https://doi.org/10.1016/j.compositesb.2016.06.031.

[10] P. Vilímová, J. Tokarský, P. Peikertová, K. M. Kutláková, and T. Plaček, "Influence of thermal and UV treatment on the polypropylene/graphite composite," *Polymer Testing*, vol. 52, pp. 46-53, 2016. https://doi.org/10.1016/j.polymertesting.2016.03.025.

[11] X. Jiang and L. T. Drzal, "Multifunctional high density polyethylene nanocomposites produced by incorporation of exfoliated graphite nanoplatelets 1: morphology and mechanical properties," *Polymer composites*, vol. 31, no. 6, pp. 1091-1098, 2010.

[12] D. Pedrazzoli, A. Pegoretti, and K. Kalaitzidou, "Synergistic effect of exfoliated graphite nanoplatelets and short glass fiber on the mechanical and interfacial properties of epoxy composites," *Composites Science and Technology*, vol. 98, pp. 15-21, 2014. https://doi.org/10.1016/j.compscitech.2014.04.019.

[13] S. N. Alam and L. Kumar, "Mechanical properties of aluminium based metal matrix composites reinforced with graphite nanoplatelets," *Materials Science and Engineering*: A, vol. 667, pp. 16-32, 2016. https://doi.org/10.1016/j.msea.2016.04.054.

[14] M. Karevan, S. Eshraghi, R. Gerhardt, S. Das, and K. Kalaitzidou, "Effect of processing method on the properties of multifunctional exfoliated graphite nanoplatelets/polyamide 12 composites," *Carbon*, vol. 64, pp. 122-131, 2013. https://doi.org/10.1016/j.carbon.2013.07.043.

[15] Y. Li, H. Zhang, H. Porwal, Z. Huang, E. Bilotti, and T. Peijs, "Mechanical, electrical and thermal properties of in-situ exfoliated graphene/epoxy nanocomposites," *Composites Part A: Applied Science and Manufacturing*, vol. 95, pp. 229-236, 2017. https://doi.org/10.1016/j.compositesa.2017.01.007.

[16] F. Wang, L. T. Drzal, Y. Qin, and Z. Huang, "Enhancement of fracture toughness, mechanical and thermal properties of rubber/epoxy composites by incorporation of graphene nanoplatelets," *Composites Part A: Applied Science and Manufacturing*, vol. 87, pp. 10-22, 2016. https://doi.org/10.1016/j.compositesa.2016.04.009.

[17] T. Rath and Y. Li, "Nanocomposites based on polystyrene-b-poly (ethylene-r-butylene)-b-polystyrene and exfoliated graphite nanoplates: effect of nanoplatelet loading on morphology and mechanical properties," *Composites Part A: Applied Science and Manufacturing*, vol. 42, no. 12, pp. 1995-2002, 2011. https://doi.org/10.1016/j.compositesa.2011.09.002.

[18] K. Kalaitzidou, H. Fukushima, and L. T. Drzal, "A new compounding method for exfoliated graphite–polypropylene nanocomposites with enhanced flexural properties and lower percolation threshold," *Composites Science and Technology*, vol. 67, no. 10, pp. 2045-2051, 2007. https://doi.org/10.1016/j.compscitech.2006.11.014.

[19] S. Kim, J. Seo, and L. T. Drzal, "Improvement of electric conductivity of LLDPE based nanocomposite by paraffin coating on exfoliated graphite nanoplatelets," *Composites Part A: Applied Science and Manufacturing*, vol. 41, no. 5, pp. 581-587, 2010. https://doi.org/10.1016/j.compositesa.2009.05.002.

[20] M. Mantilaka, H. Pitawala, D. Karunaratne, and R. Rajapakse, "Nanocrystalline magnesium oxide from dolomite via poly (acrylate) stabilized magnesium hydroxide colloids," *Colloids and Surfaces A: Physicochemical and Engineering Aspects*, vol. 443, pp. 201-208, 2014. https://doi.org/10.1016/j.colsurfa.2013.11.020.

[21] L. Shen, I. Y. Phang, L. Chen, T. Liu, and K. Zeng, "Nanoindentation and morphological studies on nylon 66 nanocomposites. I. Effect of clay loading," *Polymer*, vol. 45, no. 10, pp. 3341-3349, 2004. https://doi.org/10.1016/j.polymer.2004.03.036.

[22] A. I. Alateyah, H. N. Dhakal, and Z. Y. Zhang, "Processing, Properties, and Applications of Polymer Nanocomposites Based on Layer Silicates: A Review " *Advances in Polymer Technology*, vol. 32, no. 4, 2013. https://doi.org/10.1002/adv.21368.

[23] J. R. Rocha, K. Z. Yang, T. Hilbig, W. Brostow, and R. Simoes, "Polymer indentation with mesoscopic molecular dynamics," *Journal of Materials Research*, vol. 28, no. 21, pp. 3043-3052, 2013. https://doi.org/10.1557/jmr.2013.307.

[24] L. Shen, I. Y. Phang, T. Liu, and K. Zeng, "Nanoindentation and morphological studies on nylon 66/organoclay nanocomposites. II.

Effect of strain rate," *Polymer*, vol. 45, no. 24, pp. 8221-8229, 11// 2004.

[25] Y. Geng, S. J. Wang, and J.-K. Kim, "Preparation of graphite nanoplatelets and graphene sheets," *Journal of colloid and interface science*, vol. 336, no. 2, pp. 592-598, 2009. https://doi.org/10.1016/j.jcis.2009.04.005.

[26] P. Song, Z. Cao, Y. Cai, L. Zhao, Z. Fang, and S. Fu, "Fabrication of exfoliated graphene-based polypropylene nanocomposites with enhanced mechanical and thermal properties," *Polymer*, vol. 52, no. 18, pp. 4001-4010, 2011. https://doi.org/10.1016/j.polymer.2011.06.045.

[27] A. I. Alateyah, H. N. Dhakal, and Z. Y. Zhang, "Water absorption behaviour, mechanical and thermal properties of vinyl ester matrix nanocomposites based on layered silicate," *Polymer-Plastics Technology and Engineering*, vol. 53, pp. 1-17, 2014. https://doi.org/10.1080/03602559.2013.844246.